


**Memory of incomplete phase transitions from a random squares model**F. Țolea, M. Sofronie, M. Niță, and M. Țolea *National Institute of Materials Physics, POB MG-7, 77125 Bucharest-Magurele, Romania* (Received 25 May 2023; revised 20 October 2023; accepted 30 November 2023; published 26 December 2023)

We present a simple two-dimensional model for a phase transition, then study its predictions, in particular the memory properties. The direct transformation is modeled by randomly placing small squares, “nuclei”, on an initially empty surface. Then, the nuclei expand (“grow”) up to finite final sizes which are randomly chosen in a given range, while keeping their square shape. An important issue is the “interaction” which forces some squares to remain at smaller sizes if the surrounding squares get in the way of their growth. Interestingly, this naturally leads to quasiequal total area covered by the squares of each size after a complete direct transformation. Next, it is shown that the system “remembers” incomplete (“arrested”) reverse transformations taking place in reversed order of the squares sizes. The memory is “encrypted” in the distribution of the squares sizes after a next direct transformation and manifests as a significant imbalance between the areas covered by the “big” and “small” (relative to the arrest size) squares. We are able to also reproduce the so-called “hammer effect” and the memorizing of multiple arrest points. Our model is particularly relevant for the thermal memory effect in shape memory alloys, and we actually borrowed many features from existing thermodynamic models addressing this effect. However, here we eliminate the explicit thermodynamics and end up with a statistical geometry model, presumably easier to reproduce.

DOI: [10.1103/PhysRevE.108.064134](https://doi.org/10.1103/PhysRevE.108.064134)**I. INTRODUCTION**

Memory effects imply the existence of multiple states (ground states or metastable ones) that a system can access selectively, depending on the history acting upon them (magnetic field variations, temperature variations, etc).

Perhaps the most encountered memory effect in solid state physics is the magnetic hysteresis, when ferromagnetic materials “remember” the sense of the magnetic field variation. Similarly, the ferroelectric materials keep a memory of the electric field variation. The hysteresis loops are described in an elegant and simple manner by the purely Mathematical model of Preisach [1], based on the consideration of a large number of independent hysterons, each with a “switch up” and a “switch down” value. Subsequently, the Preisach model received various developments and was shown to apply to a wider class of phenomena (see, e.g., Refs. [2,3]).

A different kind of example is the memory of shape exhibited by the shape memory alloys (SMA), which, after being deformed can recover their initial shape by heating, applying magnetic fields, etc. This property relies on the small enthalpy difference between the austenite and martensite crystalline phases, as well as the nondiffusive nature of the phase transition; layers of atoms just slip collectively. As such, a SMA may undergo the phase transition rather than accumulate elastic stress or create defects, when acted upon. The reversibility of the phase transition implies the “remembering” of the initial shape (the literature here is vast, we indicate just some

examples [4–6], and the alloys may be, e.g., Ni-Ti, Cu-Zn-Al, Fe-Mn-Si, Cu-Al-Ni, Ni-Ti-Pd, Ni-Mn-Ga, Ti-Nb etc).

Interestingly, the SMA were shown to remember not only shapes, but also temperatures corresponding to incomplete phase transitions which happened in the past. The thermal memory effect (TME) in SMA [7–16], sometimes also named “thermal arrest”, is however less understood and received less attention so far. In short, the TME manifests as follows: A system which is initially in the martensite phase at low temperatures is warmed up to a temperature where the austenite transformation started but didn’t finish, let’s call this “arrest temperature” (AT). Next, the system is again fully cooled into martensite and finally fully heated into austenite. If one records the calorimetric signal, the heat exchange of the final martensite to austenite transformation, a dip will be noticed to a temperature close to AT.

The TME is not restricted to SMA, being also found in, e.g., FeRh, which has a first-order magnetic transition [17], suggesting that it may rely on more general principles than the particularities of the martensitic transformation. Apart from the fundamental relevance towards a better understanding, the effect may find also important practical applications [13,18].

Other works [7,9,19–22] showed that the TME also manifests as: memorizing multiple arrest temperatures, the possibility to erase the memorized temperature(s) by heating to a superior temperature, but also to an inferior close one, and the effect can be increased by repeating the arrest (“hammer effect”).

In this paper we present a simplified, purely statistical geometry version of the thermodynamic models already existing in the literature [9,10,15] which reproduced the TME. As seen from the Preisach case [1–3], mathematical models

\*tzolea@infim.ro

have high generality and ease of use. Here, a solid state phase transition is modeled by nucleation and growth of random *finite* sizes squares. Although related to, our nucleation and growth scenario differs from the much more studied random sequential absorption (RSA), see, e.g., the review [23], where the shapes (squares, circles, etc) are placed directly with their final size in an available place. While the RSA applies directly to phenomena such as adsorption of molecules, a nucleation scenario fits better the phase transition problems. Also, our scenario differs from the classical nucleation and growth, where the growth of germs only stops at the completion of the phase transition or when they meet areas already transformed (see, e.g., Refs. [24–26]).

Our approach is directly inspired by the martensitic transformation in SMA, that is known to take place by formation of finite size plates, i.e., that do not grow indefinitely, then the phase transition continues by formation of new plates, rather than further growth of the existing ones. About the reverse transformation, it will be assumed that the smaller squares transform back first (“disappear”) and the bigger ones last. Accordingly, an incomplete reverse transformation would leave the larger squares untransformed and therefore would influence the squares sizes distribution of a subsequent direct transformation, this being a memory effect discussed in detail in this paper.

The outline of the paper is as follows: In Sec. II we briefly review existing thermodynamic models capturing memory effects (TME), in Sec. III we present the features of the new statistical model, which is numerically tested in Sec. IV. Appendix A gives a toy model for the calorimetric signal of the reversed phase transition (“reading” the memory), Appendix B gives details of the numerical implementation and some additional data, while in Appendix C we briefly talk about the Palasti conjecture.

## II. EXISTING THERMODYNAMIC MODELS (1 AND 2) FOR THE TME IN SMA

In this section we briefly outline the main features of two existing thermodynamic models that predict memory effects, more precisely, the TME. These models represented the starting point of our study, and what we will do in the following sections will be to provide an alternative that is purely statistical geometry. Throughout this paper, the thermodynamic models will be called Model 1 and Model 2.

Model 1 was proposed by Rodriguez-Aseguinolaza *et al.* [9,10] and its features can be summarized:

(M1a) (*direct transformation*) The *finite size* martensite plates—formed during the austenite to martensite transformation—have different *densities of elastic energy* incorporated. The densities of elastic energy range from 0 to  $G_{el}^{max}$ .

(M1b) (*reverse transformation*) In the reverse transformation (martensite to austenite) the plates with the larger elastic energy stored are the first to transform back (“disappear”) and the plates with the smaller elastic energy transform back last.

(M1c) (*thermal memory cycle*) If a reverse transformation is stopped before completion (arrested at a temperature  $T_A$ ) the plates with the elastic energy in the interval 0 to  $G_{el}^A$

remain untransformed, while those with elastic energies in the interval  $G_{el}^A$  to  $G_{el}^{max}$  transform back (disappear). A subsequent cooling back into martensite would therefore start from this distribution of plates with elastic energy in the interval 0 to  $G_{el}^A$  plus austenite domains which will transform to martensite like the initial transformation: with elastic energies in the range 0 to  $G_{el}^{max}$ .

(M1d) (*implications*) At this point, please note that the distribution of elastic stress after (c) differs from the one from (a) in the sense that we have a larger number of plates with elastic stress in the interval 0 to  $G_{el}^A$  (those remained untransformed plus those newly formed) and a depletion of plates with elastic stress in interval  $G_{el}^A$  to  $G_{el}^{max}$ . This is a memory effect and can be “read” by a calorimetric scan when heating back to austenite.

Model 2 was proposed by ̐olea *et al.* [15] and its features can be summarized:

(M2a) (*direct transformation*) The martensite plates, formed during the austenite to martensite transformation, are modeled as squares which nucleate in random places and then grow to *intrinsic maximum sizes*, with the sides lengths in the range  $L_{min}$  to  $L_{max}$ . The “intrinsic maximum size” of the squares is assumed to decrease with temperature, while the actual size reached can be smaller due to geometrical constrictions imposed by neighboring squares. An isothermal martensitic transformation was assumed, and the speed of the cooling had an important role in the final sizes distribution.

(M2b) (*reverse transformation*) In the reverse transformation (martensite to austenite) the smaller plates are the first to transform back (“disappear”) and the larger plates transform back last.

(M2c) (*thermal memory cycle*) If a reverse transformation is stopped before completion (arrested at a temperature  $T_A$ ) the plates with sizes from  $L_A$  to  $L_{max}$  remain untransformed, while those with sizes from  $L_{min}$  to  $L_A$  transform back (disappear). A subsequent cooling back into martensite would therefore start from this distribution of plates sizes in the interval  $L_A$  to  $L_{max}$  plus austenite domains which will transform to martensite like the initial transformation: by formation of squares with sides from  $L_{min}$  to  $L_{max}$ .

(M2d) (*implications*) The distribution of plates sizes after (c) differs from the one from (a) in the sense that we have a larger number of plates with sizes in the interval  $L_A$  to  $L_{max}$  (those remained untransformed plus those newly formed) and a depletion of plates with sizes in interval  $L_{min}$  to  $L_A$ . This redistribution of plates sizes distribution is a memory effect, detectable calorimetrically.

Please note that the “size of the plate” from Model 2 plays the role of the “elastic stress density” from Model 1. A smaller plate has a higher “surface to volume” ratio and would be the first to become unstable, just like a plate with larger elastic stress. Size and stress density are therefore equivalent thermodynamically, where the two models are concerned.

## III. STATISTICAL GEOMETRY MODEL 3

We start by giving the features of the Model 3, proposed in this paper, followed by discussions and numerical simulations:

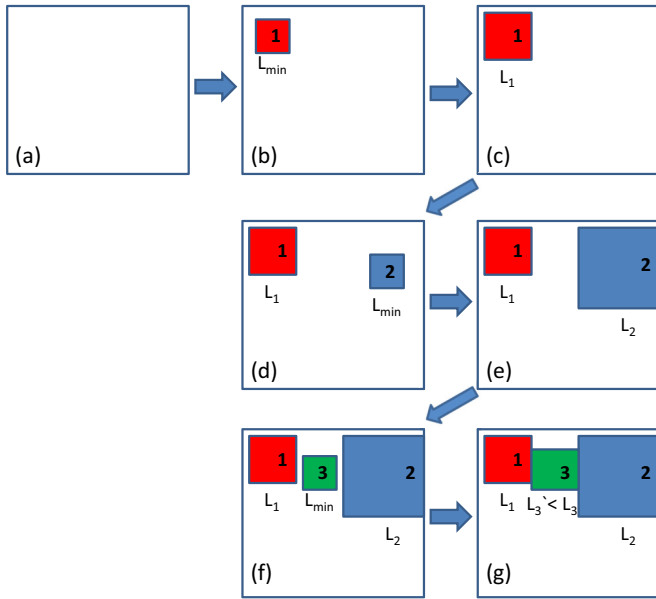


FIG. 1. Schematic description of a solid state phase transition modeled by nucleation and growth of random squares. (a) One starts from an empty surface. (b) A first square with the minimum allowed size ( $L_{\min}$ ) is randomly placed (we call this “nucleation”) and then grows (c) up to a random final size ( $L_1$ ) in the range  $L_{\min} \leq L_1 \leq L_{\max}$ . [(d)–(e)] The same happens with the second square. (f) It is possible that some squares nucleate in the vicinity of others, as square No. 3. Then let us assume that we randomly chose a final size for him  $L_3$ . (g) However, due to the geometrical constrictions imposed by the squares 1 and 2, the third square can only grow to a final size  $L'_3 < L_3$ . We call this effect “interaction between squares” and it plays an important role in the final distribution of squares sizes.

(M3a) (*direct transformation*) We model a phase transition by formation of squares which nucleate in *random* places and then grow to *randomly* chosen sizes, with the sides lengths in a given range from  $L_{\min}$  to  $L_{\max}$ . However, if the already existing neighboring squares get in the way, the new squares may grow to smaller sizes than initially chosen (“interaction” effect).

(M3b) (*reverse transformation*) In the reverse transformation, the smaller squares are the first to transform back (“disappear”) and the larger squares transform back last.

(M3c) (*memory cycle*) If a reverse transformation is incomplete, only the squares with sides in the range  $L_{\min}$  to, say,  $L_A$  transform back (disappear), while the squares with sizes from  $L_A$  to  $L_{\max}$  remain untransformed. A subsequent direct transformation would therefore start from this existing distribution of square sizes in the interval  $L_A$  to  $L_{\max}$ , then the phase transition continues with new squares formed with sides in the range  $L_{\min}$  to  $L_{\max}$ .

(M3d) (*implications*) The distribution of plates sizes after (c) differs from the one from (a) in the sense that we have a larger number of plates with sizes in the interval  $L_A$  to  $L_{\max}$  (those remained untransformed plus those newly formed) and a depletion of plates with sizes in interval  $L_{\min}$  to  $L_A$ . In particular, squares with sizes close to (but smaller than)  $L_A$  will be the fewest, due to the increased role of geometrical constrictions, see the numerical simulations below. This redistribution of squares sizes is a memory effect.

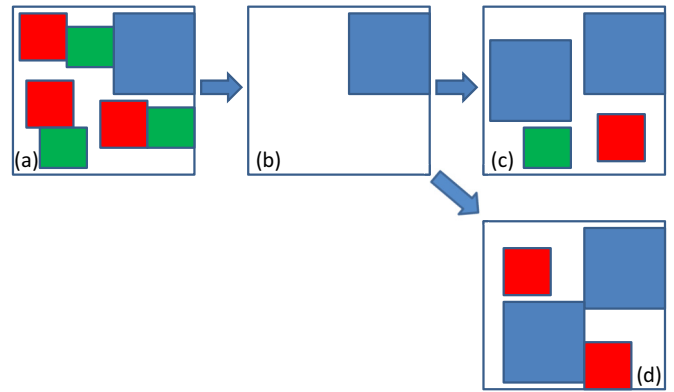


FIG. 2. Scheme of “memorizing incomplete phase transitions”. Let us assume that a “normal” phase transition—taking place by random nucleation and growth of squares, as described at (M3a)—ends up with the sizes distribution from (a). Next, an incomplete reverse phase transition transforms back the smaller red and green squares (i.e., they “disappear”) and only the big blue square survives (b). In the next direct transformation there is a probability that another big square forms nearby, such as in (c) or (d), and this only allows the formation of two more small squares, therefore a distribution different from the one in (a).

Please note that the above described model is purely geometrical and can be implemented without any knowledge of thermodynamics. We now find ourselves in the land of mathematics, although the mathematicians themselves are less interested in nucleation and growth problems, so the main use will likely stay with the physicists. In the following we discuss in detail how the new model compares with the previous ones.

The main theme presented in this paper resides in the property (M3a) which essentially differs from the previous (M2a) and (M1a) shifting the model towards statistical geometry. In Model 2, the thermodynamics was heavily involved in the property (M2a), where it was assumed that plates grow at most up to a “maximum intrinsic size” which was temperature dependent. A rather complicated phenomenological dependence was assumed, with many parameters influencing the final plates sizes distribution. For instance, because of the dependence of the intrinsic maximum size on temperature, a balanced distribution of plates sizes was obtained only for certain speed of cooling (neither too high, nor too low, which reduced the generality of the model). Instead, within the Model 3 we will now assume *random* “intrinsic maximum size” for each new plate, not related to the temperature, nor with the minimum germ size. This is a simplifying feature inspired by Model 1 (M1a) where a relatively uniform distribution of elastic stress was assumed. In our case, the randomness of sizes plus the geometrical constrictions naturally ensure uniform mass distributions, as will be shown in the numerical simulations.

As can be noticed, the newly introduced Model 3 maintains similarities with the previous Model 2 (see Sec. II). For instance, (M3d) is textually similar with (M2d), and indeed the two models can predict, in principle, similar final plates size distributions. However, the sizes distribution predicted by Model 2 depend on the thermodynamic parameters chosen, unlike the distribution predicted by Model 3. Also notice

that (M3b) and (M3c) are textually similar with (M2b) and, respectively, (M2c), however, the temperature is no longer explicitly present in Model 3.

At this point, we want to give some justification of the fact that the squares have sizes in a range from  $L_{\min}$  to  $L_{\max}$  [property (M3a)], while keeping relevance for solid state phase transitions. The existing of a minimum allowed size  $L_{\min}$  has to do with the “critical nucleation germ” concept. As the plates get smaller, the “surface to volume” ratio increases and the surface being a defect very small germs are thermodynamically unfavorable. The existing of a maximum allowed size  $L_{\max}$ , on the other hand, has to do with the experimental observation that the formed martensitic plates stop growing at a point and the phase transition continues by formation of new plates, rather than the growth of existing ones. In the experimental paper [27], for instance, one notices that the occurrence of very large plates tends to zero, thus supporting a “maximum size” assumption. Also the sequential proceeding of our phase transition (squares are placed one by one) hides the assumption that the growth of the nuclei is much faster than the formation of new ones.

Figure 1 shows in more detail how our Model 3 works [we refer here to the direct transformation, property (M3a)]. We start from an “empty” surface [Fig. 1(a)], which is gradually filled with small squares of different sizes, mimicking the plates formed during the martensitic transformation. The plates “nucleate” in random positions, meaning that we randomly place a square of the minimum size  $L_{\min}$  [as shown in Fig. 1(b) for the square labeled “1”]. Next, we chose a random final size of the square, which can be any value in the interval  $(L_{\min}, L_{\max})$ . In the case depicted in Fig. 1(c), plate No.1 grows to its final size  $L_1$ . Next, the scenario continues with the nucleation and growth of plate No. 2 (see Figs. 1(d) and 1(e), respectively). Finally, Figs. 1(f) and 1(g) exemplify another important aspect of our model: a plate (No. 3 in our case) may grow to a smaller size if existing plates are in the way. That is, it was assumed that plate no.3 should have grown to the randomly assigned size  $L_3$ , but because of geometrical constrictions from squares no. 1 and no. 2, it only grows to the final size  $L'_3 < L_3$ . This scenario has a small probability to happen in the early stages of the transformation, but becomes dominant in the late stages, near the jamming limit. Importantly, please note that the process is *sequential*, meaning that the squares are placed one at a time.

The main idea behind memorizing incomplete phase transitions is sketched in Fig. 2. Let us assume that a normal complete phase transition generates the plates distribution from Fig. 2(a), with one “big” blue square, three “intermediate size” red plates and three “small” green squares. When performing a reverse transformation, the smaller squares disappear first and the bigger ones last (property M3b), so one can end up in the situation from Fig. 2(b) with one the big blue square still standing. If one proceeds with another direct phase transition, then there is a probability that another big square is formed in the empty space, which would restrict the available place for other squares, as seen in Figs. 2(c) and 2(d). Of course, there is also the possibility of smaller squares to form, given the randomness assumed at (M3a), but after averaging large ensembles, the big plates will be more numerous after the arrest procedure than in “normal” transformations.

#### IV. NUMERICAL RESULTS

In this section, we present the results from numerical implementation of Model 3, previously introduced in Sec. III. A discrete “lattice” approach is used (see more details in Appendix B), and we start from an empty surface, a 120X120 “big square”, which is gradually filled with oriented squares, whose sides are between  $L_{\min} = 4$  and  $L_{\max} = 12$ . Figure 3 shows an instance of randomly placing the first 50 squares, while Figs. 3(e) and 3(i) show the average number of squares and, respectively, the average mass distribution after throwing the first 50 squares 100 times. By “mass” we mean the total area occupied by the squares of a certain size. Please note that the size distribution is relatively uniform, all averages in Fig. 3(e) being between 5 and 6, which was to be expected, given the assumption (M3a) that the final size of squares is randomly chosen. Figures 3(b), 3(c), and 3(d) show situations after placing 100 plates, 150 plates, and, respectively, the jamming limit. The “jamming limit” denotes the end of the phase transition, when there is no free space left to fit the smallest square of side  $L_{\min}$ . Below them, we give the average squares numbers and mass for each size. At the jamming limit we have a much larger number of small size plates and relatively much fewer big plates. This is because of the geometrical constrictions that become more and more relevant as the phase transition advances. This again, was to be expected, but what we did not expect *a priori* was that the mass distribution is relatively uniform at the jamming limit. It is a result potentially interesting in itself, which may require further analysis.

In the following, we simulate a transformation circle that generates memory. As mentioned in property (M3b), for the reverse transformation it is assumed that the smaller plates transform back (disappear) first and the big plates last. An “incomplete” reverse transformation means that squares with sides smaller than a certain value (say,  $L_a$ ) are removed, while the squares with sizes equal or bigger than  $L_a$  remain where they are. For the case depicted in Fig. 4(a), we have  $L_a = 9$ . Figures 4(c) and 4(e) can actually be regarded as details of Figs. 3(h) and 3(l), showing just the distribution of number and mass of the untransformed “big” squares. Next, a direct transformation proceeds from this point until the jamming limit is again reached. Figures 4(d) and 4(f) show the new square numbers and mass distributions, which differ significantly from the situation in Figs. 3(h) and 3(l). This is a memory effect, showing that the system remembers having passed through the mentioned incomplete reverse transformation. Notably, Fig. 4(f) shows that the largest squares that disappeared in the incomplete reverse transformation (with  $L = 8$ ) have in the end the smallest total mass, while smallest untransformed squares (with  $L = 9$ ) have the biggest mass. Additional data, corresponding to “arresting” the reverse transformation at different stages, can be found in Appendix B.

A legitimate question is how can memory effects appear in random transformations? Indeed, the direct transformation consists in spatially random placing squares of (also) random sizes. The answer may reside in the reverse transformation, which is not random but in reverse squares sizes. The details of the mass distribution after a previous arrest (lowest mass for the biggest transformed squares and higher mass for the



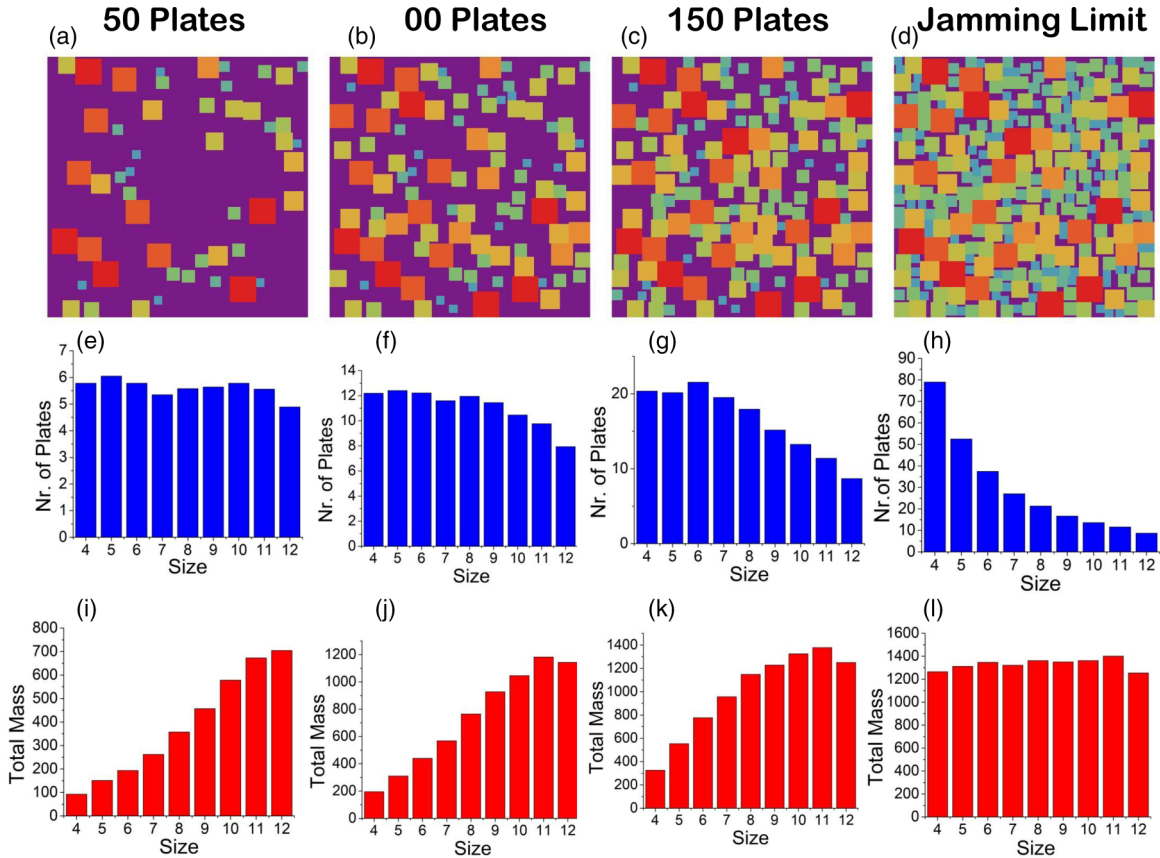


FIG. 3. Illustration of random filling of a 120X120 square (a discrete model is used) with oriented squares of sizes ranging from 4X4 to 12X12. [(a)–(d)] Example of squares spacial distribution after we randomly place the first 50, 100, 150 or all squares than can fit (jamming limit).[(e)–(h)] Plates sizes distribution after averaging over 100 realizations. [(i)–(l)] the corresponding mass distribution, i.e., total areas occupied by different sizes squares. Note that the randomness ensures uniform squares sizes distribution in early stages (e) but geometrical constrictions lead to uniform mass distribution at jamming limit (l).

smallest untransformed squares) are due to the subtle role of geometrical constrictions.

We have also performed numerical simulations for a reverse transformation in random order of the squares, regardless of their sizes (not shown here). Interesting, the system also keeps a memory of incomplete reverse transformations, manifested this time in a reduction of the big squares total area.

The Hammer effect consists in accentuating (i.e., enforcing, deepening) the memory of previous arrested transformations if the arrest procedure is repeated, similar to driving a nail deeper through successive hammer strikes. This effect has been experimentally proven for the case of thermal memory in shape memory alloys (see, e.g., Refs. [10,28] and was also numerically captured by the thermodynamic Model 1 [9,10] (described in Sec. II). In the following, we show that our statistical model also captures the hammer effect. While the experimental signature of the hammer effect would be a longer dip in the differential scanning calorimetry (DSC) signal (or a wider shoulder [10,28]), within our model we expect an even bigger imbalance in the squares distribution, and it will be shown that this indeed is the case.

To illustrate the effect with our model, we start with a “large” square of 120x120 which is randomly filled with squares in the size range  $L_{\min} = 4$  and  $L_{\max} = 20$ . One

resulting complete transformation outcome is depicted in Fig. 5(a), while the corresponding averaged squares sizes distribution is shown in Fig. 5(d). Next, an incomplete reverse transformation is performed, leaving (untransformed) only the squares with sides bigger than  $L_a = 12$ , followed by another complete direct transformation; see Fig. 5(b) for a possible spacial distribution of the squares and, respectively, Fig. 5(e) for the average distribution of sizes over 100 realizations. Finally, if the incomplete reverse transformation is repeated and another direct transformation is performed, we end up with the average distribution depicted in Fig. 5(f). We can see that the memory effect (i.e., the imbalance between the areas covered by small versus large squares) is indeed accentuated, and this is more clearly seen in Fig. 6 which plots the difference between the sizes distribution in Figs. 5(f) and 5(e). One can notice from Fig. 6 that the sizes distribution after a single and a double arrest differ mostly for the values around the arrest value (in this case  $L_a = 12$ ) and tends to zero for largest squares, respectively to low values for the smallest squares.

Double Arrest. Apart from the previously described hammer effect, it was also experimentally proven that SMA can memorize not only one but multiple temperatures at which the reverse transformation was previously stopped before completion (see, e.g., Ref. [29]).

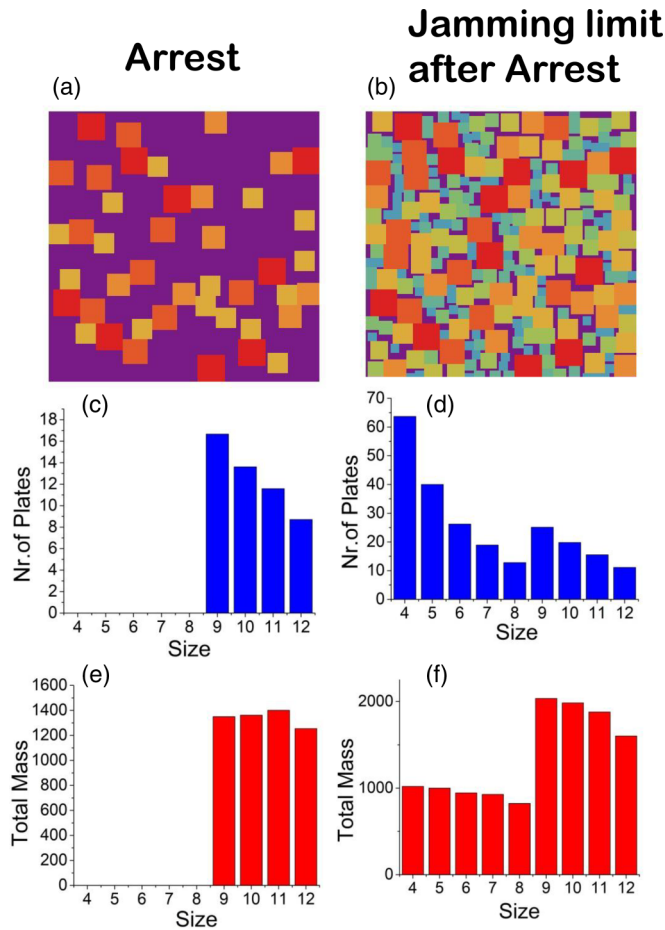


FIG. 4. (a) From the complete phase transition depicted in Fig. 3(d) we eliminated all the squares with sides smaller than 9. This mimics an incomplete reverse phase transition. (b) Then, a direct phase transition proceeds as described, by randomly placing new squares until the jamming limit. (c) and (e) Number of plates and mass distribution after the incomplete reverse transformation. (d) and (f) Number of plates and mass distribution after a new direct transformation is performed. [(c)–(f)] graphs present average values over 100 realizations.

To illustrate this with our model, we start from a  $200 \times 200$  large square which is filled as described in Sec. III with squares in the size range  $L_{\min} = 4$ ,  $L_{\max} = 20$ . One such instance is depicted in Fig. 7(a), and the averaged sizes distribution of Fig. 7(d). Next, an incomplete reverse transformation is performed, arrested at the size  $L_{a1} = 16$  followed by a direct transformation, the average distribution obtained being given in Fig. 7(e). Finally, if the next arrest procedure is done at the size  $L_{a2} = 10$ , we end up with the distribution in Fig. 7(f), showing that the system memorized both of the previous incomplete reverse transformations.

To this end, let us do a “chromatic” comparison between Figs. 7(a), 7(b), and 7(c). The bigger squares are the color red, the intermediate ones are orange-yellow-green and the smaller ones are blue, while the “untransformed” surface is purple. It is “visual” that Fig. 7(b) has “less blue” than Fig. 7(a), after the first arrest, while after the second arrest blue is even less present and the orange-yellow become dominant. Similar

chromatic differences can be found between Figs. 5(a), 5(b), 5(c) or between Figs. 4(b) and 3(d).

We have, therefore, shown that our statistical model memorizes the simple arrest but also repeated or double arrests. It is trivial that we also capture the property of “erasing” the memory after a complete reverse transformation—case in which we go back to the empty initial surface with no squares on it—while effects like “aging” (memory of multiple complete transformations) cannot be captured by our model, for the same reason.

## V. CONCLUSIONS

We describe a simple “random squares” model for a phase transition with memory properties. The direct transformation is modeled by nucleation of squares in random places, squares which then grow to (also random) final sizes, ranging between a minimum and a maximum value. The reverse transformation consists in “disappearing” of the squares in reverse size order, the smaller squares first and the larger last.

Numerical simulations have been performed on a discrete square grid, the results being summarized in the following. In the early stages of the direct transformation one has a uniform number of square with different sizes (as expected from the sizes randomness), but interestingly in the late stages one has a uniform mass distribution of the different sizes. The smaller squares become increasingly more numerous, so in the end they cover a total surface similar to the largest squares that are much fewer. This happens because of the geometrical constrictions, which play an increasing role as the number of plates increases and force the plates to stop growing at smaller and smaller sizes. The “interaction” between plates therefore plays an important role in establishing the final square size distribution.

Next, we showed that our system has memory properties, following the scenario of TME in SMA. If one performs an incomplete (“arrested”) reverse transformation, only the squares with the sides smaller than a certain value (say,  $L_A$ ) disappear, while the bigger ones remain untransformed. As such, a subsequent direct transformation will end up having an “anomalously” large number of big plates (existing plus newly formed), and a depletion of intermediate and small plates. As a detail of the numerical results, we noticed that the smallest squares untransformed in the incomplete reverse transformation will end up having the highest total mass in the end, and the largest plates transformed in the incomplete reverse transformation the smallest mass. Therefore, the system remembers not only *that*, but quite precisely *when* the reverse transition was “arrested”.

Separate numerical calculation (not presented in the paper) show that even if the reverse transformation is also random (squares randomly disappear, regardless of their sizes) the system still keeps a memory of incomplete reverse transformations, but manifested differently: after a subsequent direct transformation the total area covered by the squares of different sizes decreases uniformly with the size.

It is also shown that our statistical model can reproduce both the so called “hammer effect” and the memorizing of multiple arrest points, features that have been previously observed experimentally in the case of SMA and also captured

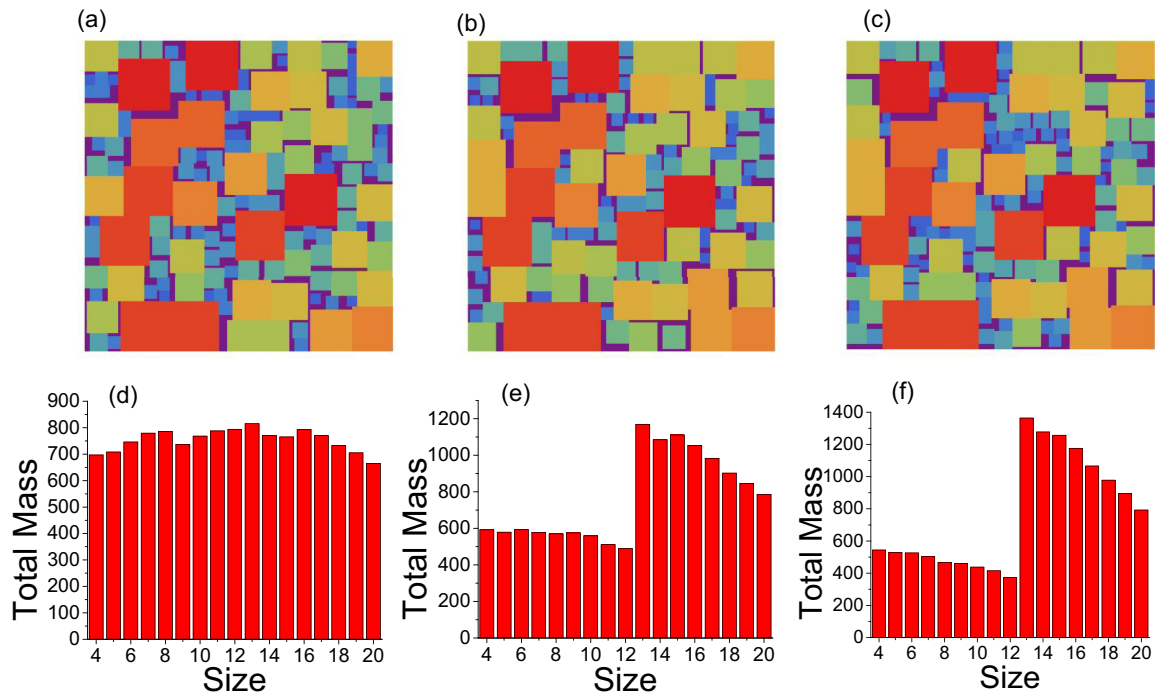


FIG. 5. Hammer effect, see description in the text. (a) A random distribution of plates after a “normal” complete direct transformation, (b) after one previous incomplete reverse transformation stopped at size 12 and (c) after repeating twice the same incomplete reverse transformation. [(d)–(e)] Total area covered by squares of different sizes for the three transformations, averaged over 100 realizations.

by the existing thermodynamic models. This proves (in our opinion) the potential of our statistical model to describe a large class of phenomena.

A toy model is given in the Appendix A showing that the mass distribution differences should be detectable by calorimetric measurements, should our model be applied to physical systems. The different distribution of plates sizes should also be detectable by microscopy or by magnetic measurements for magnetic solids.

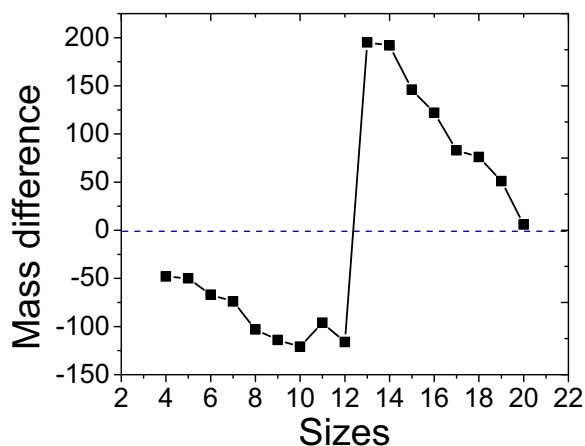


FIG. 6. Quantitative description of the Hammer effect shown in Fig. 5. The difference between the total area (mass) covered by different sizes squares after a double and, respectively, a single previous incomplete transformations (which left untransformed the squares with sides bigger than 12; i.e., the ratio per size in Figs. 5(f) versus 5(e)).

Our model borrows many features from already existing thermodynamic models which succeeded to reproduce the so-called TME in SMA (see Sec. II). Still, the novelty of random sizes squares and the absence of explicit thermodynamics shift it towards statistical geometry. Nevertheless, even if the thermodynamics is not present in an explicit way, the assumptions made do have implicit thermodynamic justification. The finite size of the squares is inspired from the finite size of the plates in the martensitic direct transformation and the reverse transformation takes place in reverse size order because smaller plates are the first to become unstable, having a larger “surface to volume” ratio. Thus, our model should be relevant for solid state phase transitions in general and for shape memory alloys in particular. In Appendix C we discuss possible relevance of our discrete model for the Palasti conjecture, which will be addressed in a future work.

#### ACKNOWLEDGMENTS

This work was supported by the Romanian Ministry of Research, Innovation and Digitization, Grants No. 35PFE/2021 and No. PN-III-P2-2.1-PED-2019-3453 (Contract No. 493/2020), and also by Core Program Project Grant No. PC2-PN23080202.

#### APPENDIX A: “READING” THE MEMORY: A TOY MODEL

Within our model, the memory of a previous incomplete transformation is “encrypted” in the changes of the square sizes distribution. Technically, this memory can be “read” by microscopy, or, as usually happens for the TME in SMA, by calorimetry measurements (DSC).

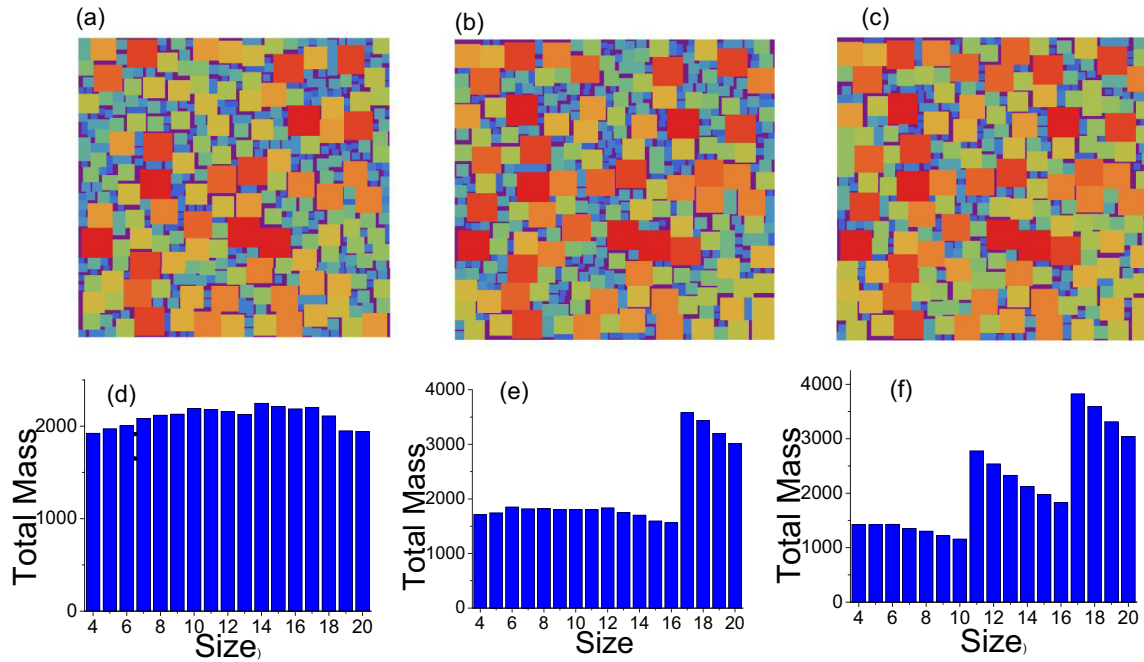


FIG. 7. Double arrest, see the description in text. (a) A random distribution of plates after a “normal” complete direct transformation, (b) after one previous incomplete reverse transformation stopped at size 16 and (c) after a second incomplete reverse transformation, this time stopped at size 10. [(d)–(f)] Total area covered by squares of different sizes for the three transformations, averaged over 100 realizations.

It is not a purpose of this paper to simulate accurately a calorimetric signal that would correspond to measuring the phase transitions described. A detailed suggestion to simulate a DSC signal for a similar “squares” system can be found in Refs. [15,22].

Just for illustration, we give below a simple toy model for simulating the DSC signal during the reverse phase transition, thus “reading” the memory stored in the distribution of plates sizes. The toy model presented in this Appendix assumes: (a) the square plates transform back in the reverse order of their sizes; the temperatures at which the plates become thermodynamically unstable increase with the plates sizes, and (b) the calorimetric signal corresponding to each plate size is a Gaussian curve, whose amplitude is proportional with the mass corresponding to that respective size.

Figure 8(a) shows a simulation of the DSC signal for a reverse transformation of a “normal” (uniform) mass

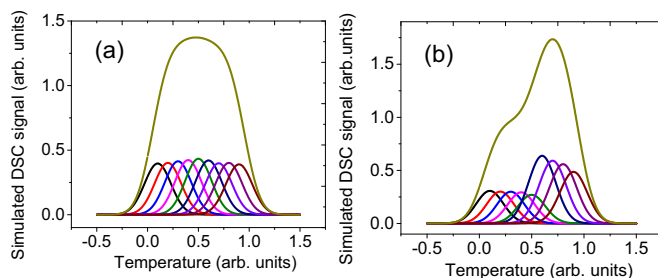


FIG. 8. Generic illustration of the way in which the memory (stored in the plates sizes distribution) may be read by a DSC calorimetry scan. (a) normal squares sizes distribution (described in Fig. 2) and (b) the squares sizes distribution after a previous incomplete reverse transformation (described in Fig. 3).

distribution of the squares sizes (such as in Fig. 3(l)), while Fig. 8(b) simulates the DSC signal of a reverse transformation after a previous arrest (such as in Fig. 4(f)). The colorful small Gauss curves in Fig. 8 simulate the DSC signals for each squares size (from  $L_{\min} = 4$  to  $L_{\max} = 12$ ), which are summed up to obtain the tall curves.

The “shoulder” noticed on the summed signal in Fig. 5(b) shows that the modified squares sizes distribution can, in principle, be detected by a calorimetric scan.

## APPENDIX B: DETAILS ON THE NUMERICAL IMPLEMENTATION AND ADDITIONAL DATA

In this Appendix we give some details on how we did the numerical implementation. As mentioned in the main text, we use a discrete model. The “nucleation” of a new plate means randomly placing a square with the smallest allowed size, let us assume  $L_{\min} = 4$ . In Fig. 9 such a minimum size square is labeled with “0”, meaning the initial size, or the “step zero in growing”. Next, our algorithm chooses a random maximum size to which this square will grow, in the range  $L_{\min} - L_{\max}$  ( $L_{\min}$  means that there is no growth, while  $L_{\max}$  is the maximum size allowed). Now, for the example depicted in Fig. 9, let us assume that the maximum size was randomly chosen to be 8. No preferential directions of growth are assumed, so we want the square to grow uniformly around the initial one. However, given the discrete model, one has to start in some direction. In Fig. 9 it is assumed that the square grows from size 4 to size 5 in the upper right direction, adding the surfaces labeled with “1”. To ensure uniform growing, the next step is expanding in the bottom left direction and becoming a size 6 square by the addition of the areas marked with “2”. The third growing is in the



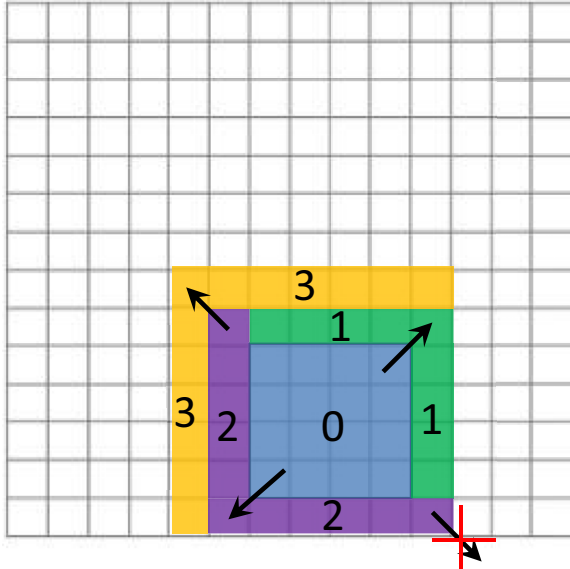


FIG. 9. Squares growth mechanism (see description in text).

upper left direction, and the square reaches size 7 by gaining the areas labeled with “3”. The next growth should be in the bottom right direction, however, this is not possible because the limits of the system have been reached. So our square from Fig. 9 will only grow to size 7, not 8 as initially chosen. The same would have happened if other pre-existing squares would come in the way, while if no geometrical constrictions are encountered the squares grow to the initially chosen maximal size.

Next, we include some additional numerical data. In the main text, Fig. 4 shows the situation after a memory circle including an incomplete reverse transformation which “made to disappear” the squares with sizes up to the value 8. We noticed that in the next direct transformation this size 8 has the smallest total mass, while the one immediately larger, size 9, has the biggest total mass (Fig. 4(f)). In general all squares with sizes 4–8 have a lower total mass than those remained untransformed, sizes 9–12. Here in, Fig. 10 we give numerical simulation for the cases when the last transformed squares have sizes from 6 to 9, to illustrate that the main conclusions hold and do not depend on the “arrest” moment (the “Total mass” in Fig. 10 is expressed in hundreds of unit cells, within our discrete model used).

In Fig. 11 we present another analysis of the memory effect keeping the arrest squares size and the maximum squares size fixes ( $L_a = 8$  and  $L_{max} = 12$ , respectively), and varying  $L_{min}$  from 1 to 6. The memory effect is clearly present in all cases, and we propose here a “quantification” of the memory effect by the ratio between the maximum and minimum areas covered by different squares. This happens to be the ratio between the area occupied by the smallest squares untransformed (in the incomplete reverse transformation) and the largest squares transformed. For the case in Fig. 11, we should do the ratio between the masses of the sizes 9 versus 8. From Fig. 11(a) to Fig. 11(f), these ratios have the values, respectively, 2.36, 2.45, 2.32, 2.41, 2.44, 2.50. We can comment that there is not a significant variation, and also the instances plotted in Fig. 10

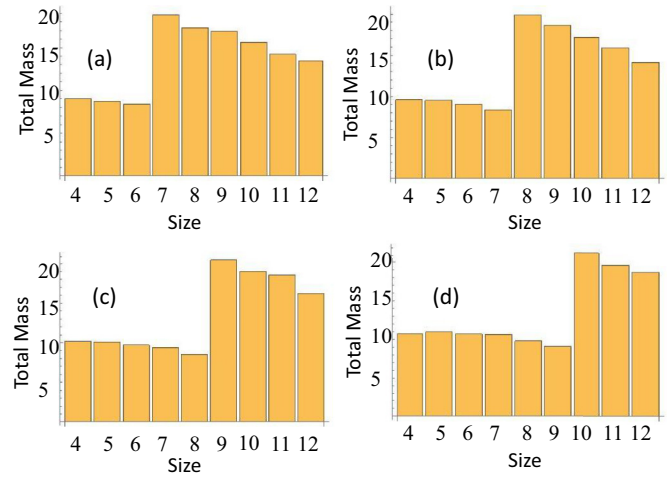


FIG. 10. Squares sizes mass distribution (see description in text) after a previous incomplete reverse transformation stopped at the squares having the sides ( $L_a$ ): (a) 6, (b) 7, (c) 8, (d) 9. For all plots, we have  $L_{min} = 4$  and  $L_{max} = 12$ .

have these ratios in the range 2.32–2.41. This is an interesting finding, suggesting a weak dependence of the memory property on the size at which the arrest was made. For the case in Fig. 5(e) the ratio around the arrest value (areas occupied by squares with side 13 versus side 12) is 2.38, similar to the above calculated values, while in Fig. 5(e), after a repeated arrest (hammer effect) the ratio grows to 3.64.

*A complete transformation.* As discussed, our simulations of phase transitions on a discrete lattice have two main parameters  $L_{min}$  and  $L_{max}$  which are the sides of the smallest and the largest squares. In the previously presented numerical results, we had  $L_{min} > 1$  (except only for the case in Fig. 11(a)), meaning in particular that there remains some surface “untransformed” where even the smallest square (of size  $L_{min}$ ) wouldn’t fit. It is generally accepted that solid state phase transitions are in general incomplete and the martensitic transformation in particular. However, there is no reason not to try  $L_{min} = 1$  in numerical calculation and see how a “complete” phase transition looks like, also in the context of the memory properties. The numerical results are given in Fig. 12, where normal and a previously arrested phase transitions are, respectively, presented. The numerical calculations were performed on a 200X200 grid and  $L_{min} = 1$  with  $L_{max} = 20$  and  $L_a = 10$ . One can conclude that the memory effect is equally present even for a complete phase transition. Also, for the un-arrested, “normal” phase transition we notice a rather low total mass for the smallest squares, which differs slightly from the more uniform distributions in the case of incomplete phase transitions.

**APPENDIX C: A FEW WORDS ABOUT THE PALASTI CONJECTURE**

This Appendix is not directly related to the main content/idea of this paper, but we include it because some readers may find it of interest and also points towards possible further directions of study.

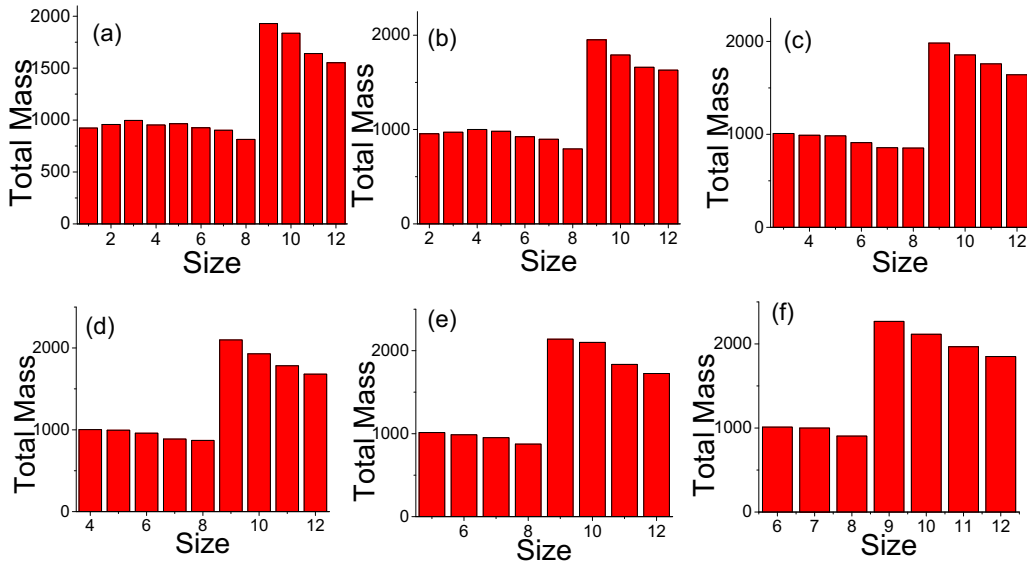


FIG. 11. Square sizes mass distribution (see description in text) after a previous incomplete reverse transformation stopped at  $L_a = 8$ , the minimum size squares  $L_{\min}$  being from 1 (a) to 6 (f). For all cases  $L_{\max} = 12$ .

Our numerical simulations were about filling a surface with random sizes squares. If instead we would have wanted to fill the surface with oriented squares of the *same* size, we would have found ourselves in the frame of Palasti conjecture [30], which can be regarded as the most famous RSA problem [23]. To briefly describe it, one should start from the one-dimensional (1D) problem, consisting of randomly placing segments of the same size on a line, also known as “car parking problem”. The same size segments are randomly placed until there is no more place for another one (i.e., all distances between segments are smaller than the segments length). The question now is: what is the average coverage? For this 1D

case there is an analytical solution (in integral form, which can be solved numerically with indefinite precision), the average covering being  $l = 0.747597\dots$ . Going to higher dimensions (d) (filling a surface with squares, a space with cubes, etc.), Palasti conjectured [30] that the average coverage is  $l^d$ . For the case of 2D, this would be  $l^2 = 0.55889\dots$

Even if some early numerical estimations [31] confirmed the Palasti conjecture within numerical margin of errors, more accurate estimations later suggest that the average coverage of a surface with oriented identical squares is  $0.5620009 \pm / - 0.000004$  [32], which is slightly higher than the Palasti value.

Our numerical simulations (an example is presented in Fig. 13) on discrete lattices and various  $l/L$  (square side

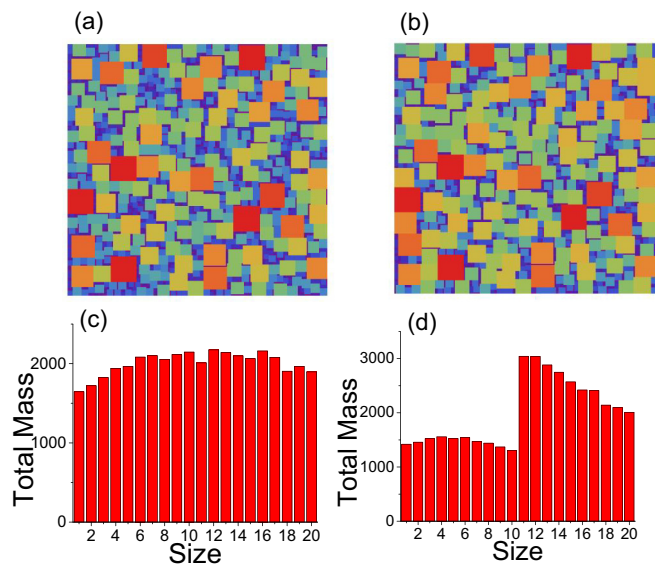


FIG. 12. (a) A “complete” direct phase transition ( $L_{\min} = 1$ ,  $L_{\max} = 20$ , on a 200x200 lattice) (b) the same after a previous arrest at  $L_a = 10$ . (c) and (d) are the respective sizes mass distribution after averaging over 200 realizations.



FIG. 13. Example of randomly filling a “big” square with the side  $L = 100$  with “small” oriented squares having the side  $l = 10$ . The small squares are randomly placed until the jamming limit is reached. In this example we could fit  $N = 54$  small squares, corresponding to 0.54 filling, while the average value we obtained was slightly less than 0.56.

versus the side of the total area to be filled) systematically yield average values above 0.55 with higher values when discretization plays a bigger role (i.e.,  $l$  is just a few lattice

constants). However, we have also finite total area effects and discretization effects, which call for a further more detailed study.

- 
- [1] F. Preisach, Uber die magnetische nachwirkung, *Z. Phys.* **94**, 277 (1935).
- [2] I. D. Mayergoyz, Mathematical models of hysteresis, *Phys. Rev. Lett.* **56**, 1518 (1986).
- [3] L. Pál, Stochastic model of hysteresis, *Phys. Rev. E* **61**, 3490 (2000).
- [4] T. Tadaki, K. Otsuka, and K. Shimizu, Shape memory alloys, *Annu. Rev. Mater. Sci.* **18**, 25 (1988).
- [5] E. Bonnot, R. Romero, L. Mañosa, E. Vives, and A. Planes, Elastocaloric effect associated with the martensitic transition in shape-memory alloys, *Phys. Rev. Lett.* **100**, 125901 (2008).
- [6] J. M. Jani, M. Leary, A. Subic, and M. A. Gibson, A review of shape memory alloy research, applications and opportunities, *Mater. Design* **56**, 1078 (2014).
- [7] G. Airoidi, A. Corsi, and R. Riva, The hysteresis cycle modification in thermoelastic martensitic transformation of shape memory alloys, *Scr. Mater.* **36**, 1273 (1997).
- [8] M. Krishnan, New observations on the thermal arrest memory effect in Ni-Ti alloys, *Scr. Mater.* **53**, 875 (2005).
- [9] J. Rodríguez-Aseguinolaza, I. Ruiz-Larrea, M. L. No, A. Lopez-Echarri, and J. San Juan, Temperature memory effect in Cu-Al-Ni shape memory alloys studied by adiabatic calorimetry, *Acta Mater.* **56**, 3711 (2008).
- [10] J. Rodríguez-Aseguinolaza, I. Ruiz-Larrea, M. L. No, A. Lopez-Echarri, and J. San Juan, A new quantitative approach to the thermoelastic martensitic transformation: The density of elastic states, *Acta Mater.* **56**, 6283 (2008).
- [11] J. Rodríguez-Aseguinolaza, I. Ruiz-Larrea, M. L. No, A. Lopez-Echarri, and J. San Juan, The influence of partial cycling on the martensitic transformation kinetics in shape memory alloys, *Intermetallics* **17**, 749 (2009).
- [12] T. Kurita, H. Matsumoto, K. Sakamoto, and H. Abe, Transformation behavior of shock-compressed Ni<sub>48</sub>Ti<sub>52</sub>, *J. Alloys Compd.* **400**, 92 (2005).
- [13] Y. Zheng, L. Cui, and J. Schrooten, Temperature memory effect of a nickel-titanium shape memory alloy, *Appl. Phys. Lett.* **84**, 31 (2004).
- [14] T. Liu, Y. Zheng, and L. Cui, Influence of partial cycling on the transformation mass of NiTi alloys, *Mater. Lett.* **112**, 121 (2013).
- [15] F. Țolea, M. Țolea, M. Sofronie, and M. Valeanu, Distribution of plates' sizes tell the thermal history in a simulated martensitic-like phase transition, *Solid State Commun.* **213-214**, 37 (2015).
- [16] G. Vitel, A. L. Paraschiva, M. G. Suru, N. Cimpoesu, and L.-G. Bujoreanu, New calorimetric structural aspects of temperature memory effect in hot rolled Cu-Zn-Al SMAs, *Optoelectr. Adv. Matter. Rapid Commun.* **5**, 858 (2011).
- [17] Y. Feng, T. Fukuda, and T. Kakeshita, Temperature memory effect associated with a first order magnetic transition in FeRh, *Intermetallics* **36**, 57 (2013).
- [18] C. Tang, T. X. Wang, W. M. Huang, L. Sun, and X. Y. Gao, Temperature sensors based on the temperature memory effect in shape memory alloys to check minor over-heating, *Sens. Actuator A Phys.* **238**, 337 (2016).
- [19] Z. G. Wang and X. T. Zu, Incomplete transformation induced multiple-step transformation in TiNi shape memory alloys, *Scr. Mater.* **53**, 335 (2005).
- [20] Z. Wang, X. Zu, and Y. Fu, Review on the temperature memory effect in shape memory alloys, *Int. J. Smart Nano Mat.* **2**, 101 (2011).
- [21] M. Z. Zhou, X. Zhang, X. L. Meng, W. Cai, and L. C. Zhao, Temperature memory effect induced by incomplete transformation in Ni-Mn-Ga-based shape memory alloy, *Mater. Today: Proc.* **2**, S867 (2015).
- [22] F. Țolea, M. Țolea, and M. Valeanu, Thermal memory fading by heating to a lower temperature: Experimental data on polycrystalline NiFeGa ribbons and 2D statistical model predictions, *Solid State Commun.* **257**, 36 (2017).
- [23] J. W. Evans, Random and cooperative sequential absorption, *Rev. Mod. Phys.* **65**, 1281 (1993).
- [24] M. Fanfoni and M. Tomellini, The Johnson-Mehl-Avrami-Kohnogorov model: A brief review, *Nuovo Cim. D* **20**, 1171 (1998).
- [25] S. E. Offerman *et al.*, Grain nucleation and growth during phase transformations, *Science* **298**, 1003 (2002).
- [26] K. Sekimoto, Generalized Avrami's formula for overlapping randomly located regions, *Phys. Lett. A* **105**, 390 (1984).
- [27] G. Ghosh, Size distribution of martensite plates in an Fe-Ni-Mn alloy, *J. Mater. Sci.* **21**, 2933 (1986).
- [28] J. Rodríguez-Aseguinolaza, I. Ruiz-Larrea, M. L. No, A. Lopez-Echarri, and J. San Juan, Thermodynamic study of the temperature memory effects in Cu-Al-Ni shape memory alloys, *J. Appl. Phys.* **107**, 083518 (2010).
- [29] J. Rodríguez-Aseguinolaza, I. Ruiz-Larrea, M. L. No, A. Lopez-Echarri, E. H. Bocanegra, and J. San Juan, Thermal history effects of Cu-Al-Ni shape memory alloys powder particles compared with single crystal behaviour, *Intermetallics* **18**, 2183 (2010).
- [30] I. Palásti, On some random space filling problems, *Magy. Tudom. Akad. Mat. Kut. Intez. Kozl.* **5**, 353 (1960).
- [31] Y. Akeda and M. Hori, Numerical test of Palásti's conjecture on two-dimensional random packing density, *Nature (London)* **254**, 318 (1975).
- [32] B. J. Brosilow, R. M. Ziff, and R. D. Vigil, Random sequential adsorption of parallel squares, *Phys. Rev. A* **43**, 631 (1991).